Atomic structure of a nanobody-trapped domain-swapped dimer of an amyloidogenic β2-microglobulin variant

Katarzyna Domanska[a,b], Saskia Vanderhaegen[a,b], Vasundara Srinivasan[a,b], Els Pardon[a,b], Florine Dupeux[c], Jose A. Marquez[c], Sofia Giorgetti[d], Monica Stoppini[d], Lode Wyns[a,b], Vittorio Bellotti[d], and Jan Steyaert[a,b,1]

[a]Department of Molecular and Cellular Interactions, Vlaams Instituut voor Biotechnologie, Pleinlaan 2, B-1050 Brussels, Belgium; [b]Structural Biology Brussels, Vrije Universiteit Brussel, Pleinlaan 2, B-1050 Brussels, Belgium; [c]Grenoble Outstation, European Molecular Biology Laboratory and Unit of Virus Host-Cell Interactions, 6 rue Jules Horowitz, BP181, 38042 Grenoble Cedex 9, France; and [d]Department of Biochemistry, University of Pavia, Via Taramelli 3b, 27100 Pavia, Italy

Edited by David S. Eisenberg, University of California, Los Angeles, CA, and approved December 6, 2010 (received for review June 17, 2010)

Atomic-level structural investigation of the key conformational intermediates of amyloidogenesis remains a challenge. Here we demonstrate the utility of nanobodies to trap and characterize intermediates of β2-microglobulin (β2m) amyloidogenesis by X-ray crystallography. For this purpose, we selected five single domain antibodies that block the fibrillogenesis of a proteolytic amyloidogenic fragment of β2m (ΔN6β2m). The crystal structure of ΔN6β2m in complex with one of these nanobodies (Nb24) identifies domain swapping as a plausible mechanism of self-association of this amyloidogenic protein. In the swapped dimer, two extended hinge loops—corresponding to the heptapetide NHVTLSQ that forms amyloid in isolation—are unmasked and fold into a new two-stranded antiparallel β-sheet. The β-strands of this sheet are prone to self-associate and stack perpendicular to the direction of the strands to build large intermolecular β-sheets that run parallel to the axis of growing oligomers, providing an elongation mechanism by self-templated growth.

crystallization chaperones | amyloid fibrils | prefibrillar intermediates | dialysis-related amyloidosis

Peptides and proteins exhibit a common tendency to assemble into highly ordered fibrillar aggregates, whose formation proceeds in a nucleation-dependent manner (1, 2). The full elucidation of the aggregation process requires the identification of all the conformational states and oligomeric structures adopted by the polypeptide chain. Atomic-level structural investigation of the key conformational intermediates of amyloidogenesis remains a challenge. This is due to the nature of the process, which may be described as a dynamic equilibrium between diverse structural species. These intermediates have dissimilar sizes and occur in very uneven amounts and time frames. Fibril formation in vivo usually takes several years, and the intermediate species are short living and highly unstable (2). Here we demonstrate the utility of heavy chain only antibodies derived from camel (3, 4) for the structural investigation of prefibrillar intermediates of β2-microglobulin (β2m) amyloidosis. The antigen-binding site of these antibodies consists of a single domain, referred to as VHH or nanobody (Nb) (4).

β2m is a 99-residue soluble protein that adopts the classical seven-stranded β-sandwich immunoglobulin fold and is expressed as a key component of the major histocompatibility class I complex (MHC-I) on the cell surface of all nucleated cells (5, 6). In healthy individuals, excess β2m is degraded and excreted from the bloodstream by the kidney. In patients suffering from renal failure, the β2m concentration increases up to 60-fold (7) leading to the formation of insoluble amyloid fibrils and causing dialysis-related amyloidosis (DRA) (8). In amyloid deposits extracted from DRA patients, up to 25–30% of the constituting β2m is truncated and lacks the six N-terminal amino acids (ΔN6β2m) (9, 10). The ΔN6-truncated form of β2m readily aggregates and fibrillates at neutral pH (10, 11).

The identification and characterization of oligomers preceding the formation of fibrils is of particular interest because of an increasing awareness that these species are likely to play a critical role in the pathogenesis of protein deposition diseases (12, 13). In this study, we selected nanobodies that block the fibrillogenesis of a proteolytic amyloidogenic ΔN6 variant of β2m. We found that one of the fibrillogenesis inhibitors traps a domain-swapped dimer of ΔN6β2m in the crystal. The crystal structure of this dimer has several properties that have been attributed to prefibrillar intermediates of β2m fibrillogenesis, providing previously undescribed insights in this process with implications for DRA.

Results

Nanobodies Efficiently Block β2m Fibrillogenesis. The use of specific antibodies offers promising strategies for inhibiting and even reversing the fibril formation by amyloidogenic proteins (4, 14, 15). The aim of this study was to generate antibodies that stabilize early intermediates along the pathway of β2m fibrillogenesis and to use these antibodies for the structural investigation of such intermediates. For this purpose, camel and llamas were immunized with β2m and ΔN6β2m. According to standard protocols, we have selected 16 nanobody clones. Eight nanobodies representing unique sequence families were chosen for further analysis. Selected nanobodies with K_d's in the nanomolar to micromolar range for β2m and ΔN6β2m variants were tested as inhibitors of ΔN6β2m fibrillogenesis (Fig. 1). Inhibition experiments were performed by incubating ΔN6β2m in the presence or absence of an equimolar amount of each nanobody. As a negative control, we also included a nanobody (Nb108) generated against another antigen. Fibrillogenesis was monitored by measuring the increase of the thioflavin T (ThT) fluorescence (16), by EM imaging, and by SDS-PAGE (Fig. 1 and Figs. S1 and S2). Considering that ΔN6β2m variant aggregates within hours, five nanobodies (Nb22, Nb23, Nb24, Nb30, and Nb272) were selected as aggregation inhibitors and tested as cocrystallization chaperones of prefibrillar intermediates.

Author contributions: K.D., E.P., M.S., L.W., V.B., and J.S. designed research; K.D., S.V., V.S., F.D., J.A.M., and S.G. performed research; K.D., V.S., E.P., J.A.M., L.W., V.B., and J.S. analyzed data; and K.D. and J.S. wrote the paper.

The authors declare no conflict of interest.

This article is a PNAS Direct Submission.

Data deposition: The coordinates of the crystal structure have been deposited with the Protein Data Bank www.pdb.org (PDB ID code 2X89).

[1]To whom correspondence should be addressed. E-mail: jan.steyaert@vib-vub.be.

This article contains supporting information online at www.pnas.org/lookup/suppl/doi:10.1073/pnas.1008560108/-/DCSupplemental.

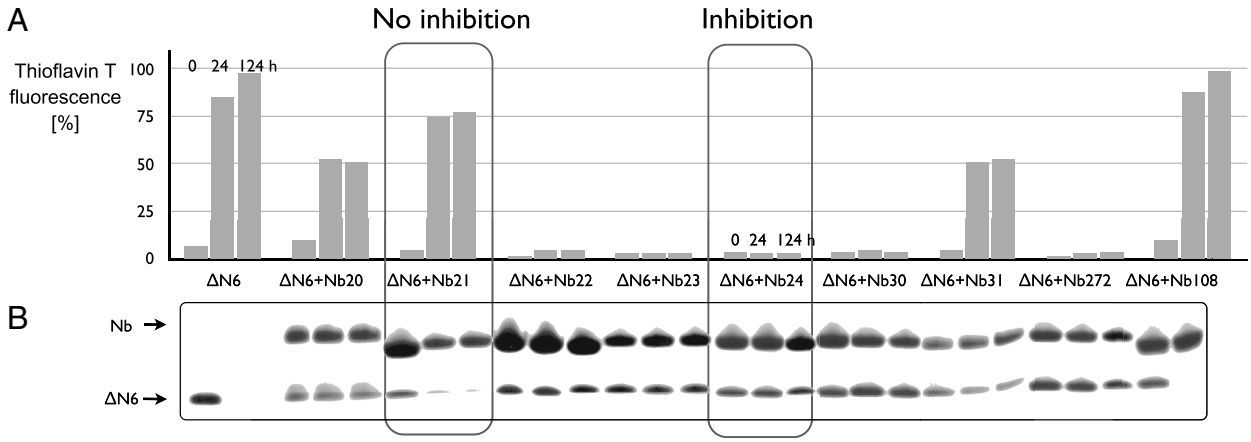

D

	Nb20	Nb21	Nb22	Nb23	Nb24	Nb30	Nb31	Nb272
K_D [nM] for β2m	24	130	269	50	58	1,6	6,8	129
K_D [nM] for ΔN6β2m	35	1500	330	54	44	6,7	8,4	72

Fig. 1. The effect of nanobodies on ΔN6β2m fibrillogenesis. ΔN6β2m (ΔN6) was incubated for one week at 37 °C in 50 mM NaAc, pH 5.0 in the absence or presence of excess amounts (42.5 μM of ΔN6β2m versus 50 μM of Nb) of nanobodies 20, 21, 22, 23, 24, 30, 31, 272, or 108 (Nb108 is a β2m-unrelated nanobody, raised against another antigen). The kinetics of fibrillogenesis were monitored by measuring the increase in ThT fluorescence after 0, 24, and 124 h (*A*). To visualize remaining soluble protein, samples were centrifuged and the soluble fractions were analyzed by SDS-PAGE (*B*). To visualize the accumulation of protein aggregates, 124-h samples were fixed on carbon-coated grids and subjected to transmission electron microscopy (*C*). Fig. S1 shows the EM images in high resolution). The table (*D*) shows the affinities of nanobodies for β2m and ΔN6β2m as measured by surface plasmon resonance.

Chaperone-Assisted Crystallization of ΔN6β2m Amyloidogenic Protein. We reasoned that antibodies inhibit protein aggregation (1) by binding to and stabilizing native or native-like states of the protein (2), by kinetically trapping early intermediates, or (3) by sterically hindering the formation of large oligomers (15). Therefore, we tested five aggregation-inhibiting nanobodies as cocrystallization chaperones for prefibrillar intermediates of β2m amyloidosis. Nanobody–antigen complexes with a molecular weight of a 1 : 1 heterodimer were obtained by mixing the purified components followed by calibrated size exclusion chromatography in a 20 mM Tris buffer containing 100 mM NaCl at pH 7.5. Despite extensive screening, diffracting crystals were obtained only from ΔN6β2m-Nb24 complex with the hanging drop vapor diffusion method using 0.2 M ammonium sulphate and 6% PEG 4000 as the precipitants in 0.1 M sodium acetate (pH 4.6). Free nanobody did not crystallize under the same conditions and purified ΔN6β2m aggregated within minutes under the crystallization conditions, indicating that the nanobody serves as an efficient crystallization chaperone for the intrinsically unstable ΔN6β2m variant. Low temperature X-ray diffraction data of the crystallized ΔN6β2m-Nb24 complex extended to 2.2 Å resolution (Table S1). The coordinates of full-length monomeric β2m (1BMG) were used as a search model to solve the crystal structure of ΔN6β2m by molecular replacement. Remarkably, the asymmetric unit of the crystal contains four molecules of ΔN6β2m, but only three nanobodies bound to three ΔN6β2m molecules (Fig. S3). As the nanobodies are fairly stable and the ΔN6β2m-Nb24 complex was purified as a 1 : 1 complex by analytical gel filtration, we exclude the possibility that one of the nanobodies was proteolytically removed during crystallization. We favor a second explanation and believe that the fourth Nb24 is present but highly mobile. There is enough space in the crystal lattice to accommodate it (Fig. S3), and we observe residual density in the area where we would expect the fourth nanobody to bind, especially in the area of ΔN6β2m-Nb interface. Partial occupancies of whole protein domains (17) or entire proteins (18) have previously been observed in crystal lattices of other protein-protein complexes.

Nb24 Stabilizes a 3D Domain-Swapped Dimer of ΔN6β2m. The crystal structure of ΔN6β2m-Nb24 complex reveals that ΔN6β2m exchanged identical subdomains between two monomers to form a 3D swapped dimer. Each domain is composed of six β-strands contributed by one subunit (A, B, E, C, D, and F) and one swapped C-terminal β-strand (strand G: residues 91–94, β2m numbering) contributed by the other (Fig. 2*B*). The short NHVTLSQ peptide (residues 83–89) serves as the hinge loop. In the monomer, the closed conformation of the hinge loop connects strands F and G. In the domain-swapped dimer the hinge adopts an extended conformation, lengthening the F strand by four amino acids (Fig. 2*F*). The extended hinge loops form a new long two-stranded antiparallel β-sheet, interrupted only by Pro90 (Fig. 2*F*). The main chain NH and CO groups of His84, Thr86, and Ser88 are hydrogen-bonded to the carbonyls and the amides of Ser88, Thr86, and His84 on the adjacent strand, respectively (Fig. 2*D*). The backbone donor and acceptor sites of Val85 and Leu87 are exposed to solvent (indicated by arrows on Fig. 2*D*), prone to stack with other β-strands in a parallel or antiparallel configuration.

Nb24 Disrupts β2-Microglobulin Aggregates in Vitro but Does not Disrupt the Fibrils. We also investigated whether Nb24 can disrupt preformed ΔN6β2m aggregates or fibrils in vitro. Therefore, 45 μM of monomeric ΔN6β2m was incubated at pH 5.0 in the presence of ThT, and fibrillogenesis was followed by electron microscopy imaging and by measuring the ThT fluorescence increase (Fig. S4). After 5 h of incubation the ThT fluorescence was no longer increasing. EM imaging confirmed the presence of nonamorphous aggregates, but no amyloid fibrils were observed at this time point (Fig. S4*A*). Those nonamorphous protein ag-

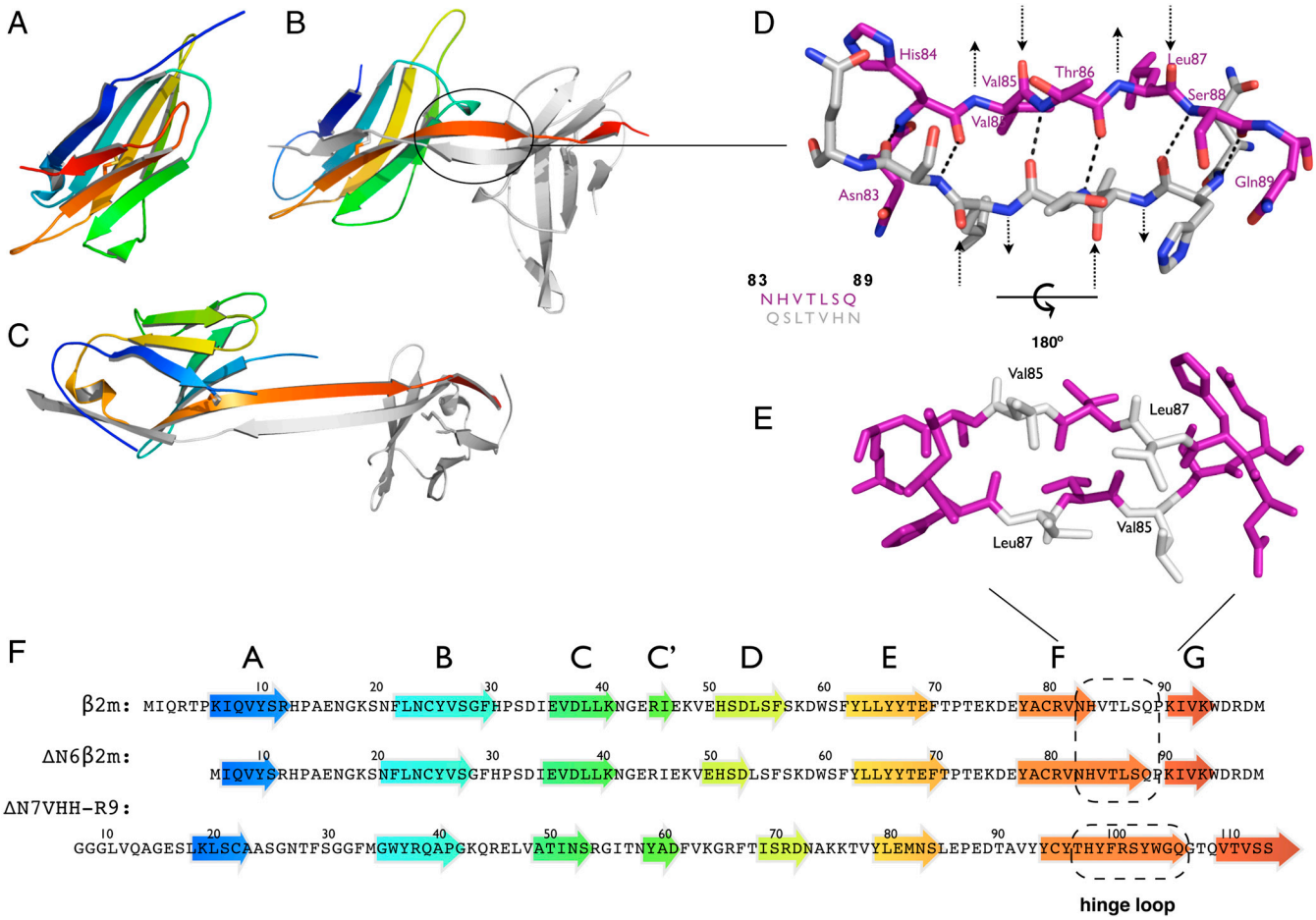

Fig. 2. Primary, secondary, tertiary, and quaternary structures of the β2m monomer compared to the domain-swapped dimers of ΔN6β2m and ΔN7VHH-R9. Ribbon representations of (*A*) the β2m monomer (1LDS), (*B*) the domain-swapped dimer of ΔN6β2m (this paper), and (*C*) the domain-swapped dimer of ΔN7VHH-R9 (1SJV). β-strands are colored according to *F*. The conserved disulfide bond that bridges the two sheets of the central β-sandwich are given in stick representation. (*D*) Structure of the open interface of ΔN6β2m dimer, showing the atomic structure for residues 83–89 of both molecules of the dimer. The main chain NH and CO groups of His84, Thr86, and Ser88 are hydrogen-bonded to the carbonyls and the amides of Ser88, Thr86, and His84 on the adjacent strand, respectively. The backbone donor and acceptor sites of Val85 and Leu87 are exposed to solvent (indicated by arrows in *D*). (*E*) Schematic representation of the hinge showing the hydrophobic patch that is exposed upon forming the new β-sheet. (*F*) Sequences and topology diagrams of β2m, domain-swapped ΔN6β2m and domain-swapped ΔN7VHH-R9. The hinge loops are included in dashed boxes.

gregates bind thT resulting in increased sample fluorescence (Fig. S4*B*). Under these conditions, the ΔN6β2m amyloid fibrils form only after two to four weeks of incubation (Fig. S2). Addition of Nb24 to preformed nonamorphous ΔN6β2m aggregates (obtained after 5 h of incubation at 37 °C and pH 5.0) caused a significant decrease of the ThT fluorescence (Fig. S4*B*) concomitant with an increase of resolubilized ΔN6β2m as shown by SDS-PAGE analysis of the soluble fraction (Fig. S4*C*). To investigate the stoichiometry of this reaction, ΔN6β2m aggregates were mixed with Nb24 at ΔN6β2m:Nb ratios of 1:1 and 4:1. Equimolar amounts of ΔN6β2m and nanobody were needed to completely disrupt the preformed ΔN6β2m fibrils, as indicated by the reduction of the ThT fluorescence to background levels. The β2m-unrelated Nb108 did not interfere with ΔN6β2m aggregation (Fig. S4*B*). We have also grown amyloid fibrils of β2m and ΔN6β2m and found that these fibrils in contrast to aggregates are stable for days in the presence of excess amounts of Nb24 (Fig. S5).

Nb24 Does not Bind the MHC-I Complex. The potency of Nb24 to recognize β2m in the MHC-I was evaluated by FACS. A series of nanobodies raised against monomeric β2m were conjugated with phycoerythrin and incubated with two human cell lines expressing MHC-I on their surface. Remarkably, most of the nanobodies, including Nb24, did not bind to MHC-I, exposed on the surface of these cells (Fig. S6).

Discussion

Many proteinaceous aggregates form through a nucleation mechanism followed by a self-templated growth where the ends of existing filaments recruit soluble molecules into aggregates (13). Consistent with this model, the assembly of β2m into amyloid-like fibrils is characterized by an initial lag phase where little or no change in fibril concentration can be detected (19). This is followed by an elongation phase where a large mass percentage of the starting protein material is converted into fibrils. The lag phase can be shortened or ultimately abolished in vitro by adding fibrillar seeds or by using designed unstable mutants (13, 15, 20). The isolation and characterization of the oligomeric species that are present in solution prior to the appearance of fibrils remains a challenge. In this work, we have trapped and characterized the structure of an amyloidogenic β2m variant that lacks six N-terminal amino acids. The crystal structure of ΔN6β2m in complex with Nb24 identifies a swapped dimer as a plausible structural nucleus that may serve as a mold for the self-templated growth of β2m fibrils (Fig. 3)

Domain Swapping Generates a Plausible Nucleus for β2m Fibrillogenesis. Three-dimensional domain swapping has been proposed as a

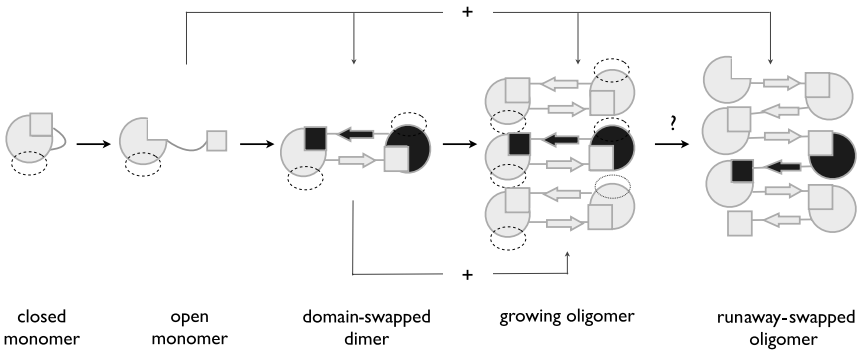

Fig. 3. Cartoon depicting possible intermediates of β2m fibrillogenesis. The self-association of two β2m monomers by domain swapping generates a dimeric intermediate with an exposed stacking prone antiparallel β-sheet. The domain-swapped dimer serves as a structural nucleus for intermolecular β-sheets that run parallel to the axis of the growing oligomer by templating the hydrogen-bonding network connecting the strands. Within the oligomer, a transition from stacked dimers to a runaway domain-swapped oligomer can lead to open ended protofibrils that grow by binding open monomers. The ends of growing oligomers can recruit open monomers or swapped dimers by a mechanism of self-templated growth. The dashed circle on the core domain of β2m represents a conceivable epitope of a nanobody that blocks aggregation by sterically hindering the self-templated growth of the swapped nucleus, thus preventing its elongation.

general mechanism for the self-association of proteins (21, 22). The ΔN6β2m dimer we trapped with Nb24 meets all common properties of domain-swapped oligomers (23). First, only one small C-terminal segment of the protein (the rest retaining the native-like structure) participates in the oligomerization, without disrupting the core of the protein fold. Second, the single disulfide bond (Cys25-Cys80) does not need to be broken to swap the domains. Finally, all sites of local perturbation that have been related to β2m self-association colocalize with the hinge region at one end of the immunoglobulin fold opposite to the nanobody binding site (Fig. 4). Most remarkably, this swapped dimer meets many characteristics that have been attributed to prefibrillar intermediates of β2m fibrillogenesis. Phe30, His31, and Pro32—three residues particularly involved in amyloidogenesis—are located on the tip of the first loop that connects strands B and C. In the native β2m monomer Pro32 adopts the *cis* conformation and makes hydrophobic contacts with the hinge loop and the N-terminal segment. Using NMR and mutagenesis, Radford and co-workers (24, 25) identified a specific folding intermediate that contains a nonnative *trans*-Pro32 isomer as a direct precursor of dimeric species and oligomers that accumulate before the development of amyloid fibrils. Using Cu^{2+} as an oligomerization trigger, Miranker and co-workers (26) also identified the *cis* to *trans* isomerization at Pro32 concomitant with a dramatic rotation of Phe30 from the hydrophobic core toward solvent as critical switches enabling aggregation. Consistent with these findings, Pro32 adopts the *trans* conformation and Phe30 takes a solvent exposed position in the swapped dimer (Fig. 4*B*). Cu^{2+} coordination at His84 contained in the hinge loop itself also induces structural rearrangements of β2m, freeing its C terminus and allowing the formation of a domain-swapped dimer (27). In the native monomer, parts of all three connecting loops are shielded from solvent by the N-terminal peptide that is missing in ΔN6β2m variant, explaining why the truncated species is less stable—and unlike wild-type protein—has a higher tendency to self-associate and forms amyloid fibrils even at physiological pH (10, 28). The different sites of local perturbation that cause the onset of β2m fibrillogenesis define the local environment of the hinge loop. It thus appears that partial unfolding at one end of the rigid β-sandwich causes the formation of fibrils via a domain-swapped intermediate that forms upon refolding of the hinge loops. The Pro32 *cis* to *trans* switch and the dramatic rotation of Phe30 are key structural signatures of this transition.

Under physiological conditions, Nb24 forms a stable nanomolar 1:1 complex with ΔN6β2m. Because Nb24 was generated in vivo by immunization with the native monomer and cloned by library selection against the same protein, it is very likely that it binds one of the lowest energy states of β2m. Thermodynamically, antibodies pay a huge energetic penalty if they first bind to a low energy state and then distort the antigen's structure into a

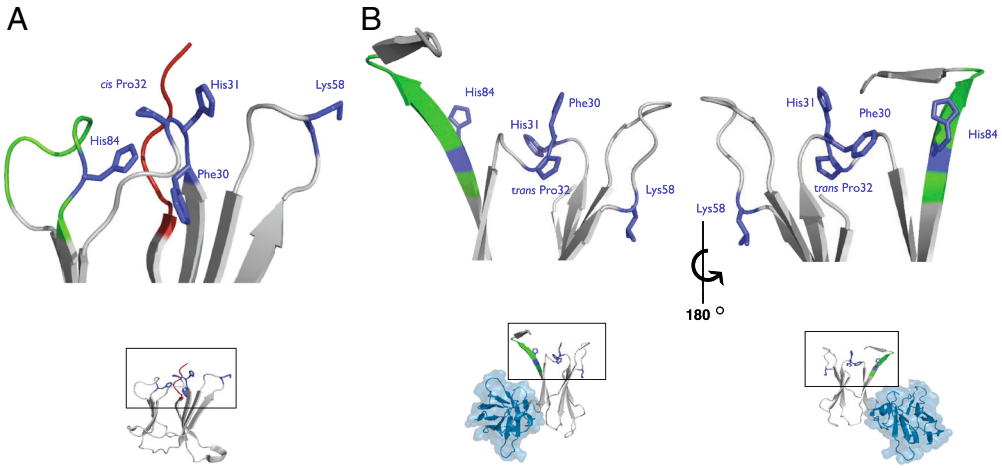

Fig. 4. Structural differences between the monomeric β2m (1LDS) and the domain-swapped ΔN6β2m dimer. Sites of local conformational flexibility associated with the formation of an early amyloidogenic intermediate are highlighted in the β2m monomer (*A*) and in the domain-swapped ΔN6β2m dimer (*B*). The hinge loop is colored in green throughout; side chains of key residues that have been implicated in the onset of multimerization are represented in blue. The N-terminal segment is highlighted in red in the β2m monomer (*A*). In ΔN6β2m-Nb24 complex, the nanobody is highlighted by its surface representation.

high-energy conformation that does not appreciably exist in the absence of the bound antibody (29). Consistently, Nb24 does not distort the structure of β2m upon binding (Fig. S7). It thus appears that the self-association step follows a gain-of-interaction mechanism (30) where an extensive portion of the native structure of the monomer (including the Nb24 epitope) is maintained in the dimer.

The Swapped Dimer Is Predisposed to Elongation by a Mechanism of Self-Templated Growth. During the self-association of ΔN6β2m, two hinges that correspond to the heptapeptide NHVTLSQ, refold into extended β-strands, and stack into a unique two-stranded antiparallel β-sheet (Fig. 2). Interestingly Ivanova et al. (31) showed that the NHVTLSQ heptapeptide forms amyloids in isolation demonstrating that this peptide by itself has a high propensity to form amyloid structure upon exposure. In the newly formed two-stranded sheet, the backbone donor and acceptor sites of Val85 and Leu87 are exposed to solvent (Fig. 2*D*), prone to stack with other β-strands in a parallel or antiparallel configuration. Indeed, other strands may associate perpendicular to build large intermolecular β-sheets that run parallel to the axis of the growing oligomers (Fig. 3). It thus appears that the swapped dimer can serve as a structural nucleus for the growth of the cross-β spine of elongating fibrils by templating the hydrogen-bonding network connecting the strands. In 3D-swapped ΔN6β2m (this study), the refolded adjacent β-strands expose a hydrophobic patch (Fig. 2*E*). This "dry surface" may provide the driving force for β-sheets of growing oligomers to associate and interdigitate. The remaining core domains may decorate the spine and protect it from solvent. In the growing oligomer, a transition from stacked swapped dimers to a runaway domain swap—where each monomer swaps a domain into the next monomer along the fibril—could generate more stable open ended protofibrils (Fig. 3). Remarkably, a llama nanobody (VHH-R9) missing the first seven amino acids was found to self-associate and stack following a similar mechanism (32). In the crystal structure of ΔN7VHH-R9, the last β-strand of the immunoglobulin fold associates with a symmetry-related molecule to form a domain-swapped dimer, its CDR3 loop refolds to generate a unique two-stranded β-sheet (Fig. 2*C*). In the packing of ΔN7VHH-R9 crystal, these two-stranded β-sheets stack with symmetry-related molecules to build a crystal-wide β-sheet structure. There is evidence that such a cross-β spine with a domain swap is also present in a designed ribonuclease A (33).

Relevance to DRA? Is a domain-swapped dimer of ΔN6β2m physiologically relevant, or is it just a crystallographic artifact? In general, domain-swapped oligomers are obtained at high protein concentrations or at low pH. Other domain-swapped proteins are fragments of their complete molecules (34). Strikingly, the deposition of β2m amyloid in humans has been correlated to high protein concentrations, lower pH, and proteolysis. First, the concentration of β2m increases up to 60-fold in the body fluids of patients suffering from DRA as an inevitable consequence of long-term hemodialysis (7). Second, the deposits of β2m are mainly localized at inflammatory sites in the muscle skeletal system. The pH of the extracellular fluids in these inflammatory loci is known to be acidic. The induction of chronic inflammation only is sufficient to trigger β2m-amyloidosis (35, 36). Third, 25% or more of the β2m in these deposits is of ΔN6-truncated form (10). Finally, it has been shown that the addition of tiny amounts of ΔN6 to β2m rapidly leads to the formation of large aggregates, suggesting that this species can serve as seeds for β2m fibrillation (28). All this points to a domain-swapped ΔN6β2m dimer as a building block of the structural nucleus of amyloid formation in DRA. High protein concentrations and a low pH may be the triggers for its formation. However, it remains to be proven if the swapped dimer is kinetically and mechanistically constructive in the process.

Stabilization of Conformational Intermediates as a Therapeutic Strategy. Different explanations may account for the antiamyloidogenic properties of Nb24. Most probably, binding of the nanobody to the core domain of β2m sterically hinders the self-templated growth of the swapped intermediate (Fig. 3), thus preventing elongation. This is consistent with our observation that Nb24 can reverse the elongation phase of β2m nuclei (Fig. S3). If the recruitment of soluble molecules at the ends of existing oligomers is reversible, nanobodies that bind the interacting interface will decompose growing fibrils by mass action. Theoretically, it cannot be excluded that the elongation of the fibrils involves structural changes in the core domain of β2m, which may be prohibited by the binding of particular nanobodies.

Using FACS, we found that Nb24 does not bind MHC-I on the cell surface (Fig. S6). It thus appears that the selected nanobody efficiently blocks the fibrillation of ΔN6β2m, without interfering with the biological function of β2m suggesting that antibodies that stabilize particular oligomeric intermediates could be developed as therapeutic tools to prevent amyloid deposits in dialysis patients.

Materials and Methods

Generation and Selection of Nanobodies. One camel (*Camelus dromedarius*) and one llama (*Llama glama*) were immunized with recombinant full-length β2m, and another llama was immunized with recombinant ΔN6β2m. From each animal, an independent phage display library was constructed. Nb20, Nb21, Nb22, and Nb24 are nanobodies derived from camel and selected against β2m. Nb23, Nb30, and Nb31 derive from ΔN6β2m-immunized llama and Nb272 originate from the llama immunized with β2m. All selected nanobodies were recloned to the pHEN6 (37) vector for expression in *Escherichia coli* as C-terminal His_6-tagged proteins. Nanobodies were purified to homogeneity by immobilized-metal affinity chromatography and gel filtration (38).

Crystallization and Data Collection. Nanobody–antigen complexes were obtained by mixing the purified components followed by calibrated size exclusion chromatography in a 20 mM Tris buffer containing 100 mM NaCl at pH 7.5. Crystals were grown at 10 °C by mixing equal volumes of protein with a reservoir solution containing 0.2 M ammonium sulfate and 6% PEG 4000 in 0.1 M Na acetate pH 4.6. The selenium–methionine labeled Nb24 produced isomorphous crystals in complex with ΔN6β2m. All X-ray diffraction data were collected at the European Synchrotron Radiation Facility (ESRF) beamlines ID29 and BM16. Crystal diffracted to 2.16 Å and a complete dataset was collected. The selenium–methionine labeled protein crystals diffracted not beyond 3.5 Å. All data were indexed, integrated, and scaled using Denzo and Scalepack (39). Subsequent data analysis was performed using the CCP4 suite of programs (40).

A detailed description of the methods can be found in *SI Materials and Methods*.

ACKNOWLEDGMENTS. We acknowledge the work of Maja Debulpaep, who performed EM imaging and the use of the beamlines at the ESRF. This work was supported by grants from the Interuniversity Attraction Poles (project P6/19), the Ministero dell'Istruzione, dell'Università e della Ricerca (Fondo per gli Investimenti della Ricerca di Base and Programmi di Ricerca di Interesse Nazionale), the European Union Framework 6 EURAMY Amyloidosis in Europe (project LSHM-CT-2005-037525) and Fondazione Cariplo and Regione Lombardia. K.D. and S.V. received doctoral fellowships of the Fonds Wetenschappelijk Onderzoek and the Innovatie door Wetenschapen Technologie, respectively.

1. Auer S, Dobson CM, Vendruscolo M, Maritan A (2008) Self-templated nucleation in peptide and protein aggregation. *Phys Rev Lett* 101:258101.
2. Harper JD, Lansbury PT, Jr (1997) Models of amyloid seeding in Alzheimer's disease and scrapie: Mechanistic truths and physiological consequences of the time-dependent solubility of amyloid proteins. *Annu Rev Biochem* 66:385–407.
3. Hamers-Casterman C, et al. (1993) Naturally occurring antibodies devoid of light chains. *Nature* 363:446–448.
4. Muyldermans S, Cambillau C, Wyns L (2001) Recognition of antigens by single-domain antibody fragments: The superfluous luxury of paired domains. *Trends Biochem Sci* 26:230–235.

5. Bjorkman PJ, et al. (1987) Structure of the human class I histocompatibility antigen, HLA-A2. *Nature* 329:506–512.
6. Trinh CH, Smith DP, Kalverda AP, Phillips SE, Radford SE (2002) Crystal structure of monomeric human beta-2-microglobulin reveals clues to its amyloidogenic properties. *Proc Natl Acad Sci USA* 99:9771–9776.
7. Floege J, Ehlerding G (1996) Beta-2-microglobulin-associated amyloidosis. *Nephron* 72:9–26.
8. Gejyo F, et al. (1985) A new form of amyloid protein associated with chronic hemodialysis was identified as beta 2-microglobulin. *Biochem Biophys Res Commun* 129:701–706.
9. Giorgetti S, et al. (2007) Lysine 58-cleaved beta2-microglobulin is not detectable by 2D electrophoresis in ex vivo amyloid fibrils of two patients affected by dialysis-related amyloidosis. *Protein Sci* 16:343–349.
10. Esposito G, et al. (2000) Removal of the N-terminal hexapeptide from human beta2-microglobulin facilitates protein aggregation and fibril formation. *Protein Sci* 9:831–845.
11. Jones S, Smith DP, Radford SE (2003) Role of the N and C-terminal strands of beta 2-microglobulin in amyloid formation at neutral pH. *J Mol Biol* 330:935–941.
12. Stefani M, Dobson CM (2003) Protein aggregation and aggregate toxicity: New insights into protein folding, misfolding diseases and biological evolution. *J Mol Med* 81:678–699.
13. Chiti F, Dobson CM (2006) Protein misfolding, functional amyloid, and human disease. *Annu Rev Biochem* 75:333–366.
14. Glabe CG (2004) Conformation-dependent antibodies target diseases of protein misfolding. *Trends Biochem Sci* 29:542–547.
15. Dumoulin M, Dobson CM (2004) Probing the origins, diagnosis and treatment of amyloid diseases using antibodies. *Biochimie* 86:589–600.
16. Levine H (1995) Thioflavine-T interaction with amyloid beta-sheet structures. *Amyloid* 2:1–6.
17. Meyer S, et al. (2009) Kissing G domains of MnmE monitored by X-ray crystallography and pulse electron paramagnetic resonance spectroscopy. *PLoS Biol* 7:e1000212.
18. Gotthardt K, Weyand M, Kortholt A, Van Haastert PJ, Wittinghofer A (2008) Structure of the Roc-COR domain tandem of C. tepidum, a prokaryotic homologue of the human LRRK2 Parkinson kinase. *EMBO J* 27:2239–2249.
19. Xue WF, Homans SW, Radford SE (2008) Systematic analysis of nucleation-dependent polymerization reveals new insights into the mechanism of amyloid self-assembly. *Proc Natl Acad Sci USA* 105:8926–8931.
20. Jarrett JT, Lansbury PT, Jr (1993) Seeding "one-dimensional crystallization" of amyloid: A pathogenic mechanism in Alzheimer's disease and scrapie? *Cell* 73:1055–1058.
21. Liu Y, Hart PJ, Schlunegger MP, Eisenberg D (1998) The crystal structure of a 3D domain-swapped dimer of RNase A at a 2.1-A resolution. *Proc Natl Acad Sci USA* 95:3437–3442.
22. Janowski R, et al. (2001) Human cystatin C, an amyloidogenic protein, dimerizes through three-dimensional domain swapping. *Nat Struct Biol* 8:316–320.
23. Liu Y, Gotte G, Libonati M, Eisenberg D (2002) Structures of the two 3D domain-swapped RNase A trimers. *Protein Sci* 11:371–380.
24. Jahn TR, Parker MJ, Homans SW, Radford SE (2006) Amyloid formation under physiological conditions proceeds via a native-like folding intermediate. *Nat Struct Mol Biol* 13:195–201.
25. Eichner T, Radford SE (2009) A generic mechanism of beta2-microglobulin amyloid assembly at neutral pH involving a specific proline switch. *J Mol Biol* 386:1312–1326.
26. Calabrese MF, Eakin CM, Wang JM, Miranker AD (2008) A regulatable switch mediates self-association in an immunoglobulin fold. *Nat Struct Mol Biol* 15:965–971.
27. Eakin CM, Attenello FJ, Morgan CJ, Miranker AD (2004) Oligomeric assembly of native-like precursors precedes amyloid formation by beta-2 microglobulin. *Biochemistry* 43:7808–7815.
28. Piazza R, et al. (2006) Micro-heterogeneity and aggregation in beta2-microglobulin solutions: Effects of temperature, pH, and conformational variant addition. *Eur Biophys J* 35:439–445.
29. Koide S (2009) Engineering of recombinant crystallization chaperones. *Curr Opin Struct Biol* 19:449–457.
30. Eisenberg D, et al. (2006) The structural biology of protein aggregation diseases: Fundamental questions and some answers. *Acc Chem Res* 39:568–575.
31. Ivanova MI, Thompson MJ, Eisenberg D (2006) A systematic screen of beta(2)-microglobulin and insulin for amyloid-like segments. *Proc Natl Acad Sci USA* 103:4079–4082.
32. Spinelli S, et al. (2004) Domain swapping of a llama VHH domain builds a crystal-wide beta-sheet structure. *FEBS Lett* 564:35–40.
33. Sambashivan S, Liu Y, Sawaya MR, Gingery M, Eisenberg D (2005) Amyloid-like fibrils of ribonuclease A with three-dimensional domain-swapped and native-like structure. *Nature* 437:266–269.
34. Liu Y, Eisenberg D (2002) 3D domain swapping: As domains continue to swap. *Protein Sci* 11:1285–1299.
35. Lardner A (2001) The effects of extracellular pH on immune function. *J Leukocyte Biol* 69:522–530.
36. Fukunishi S, Yoh K, Kamae S, Yoshiya S (2007) Beta 2-microglobulin amyloid deposit in HLA-B27 transgenic rats. *Mod Rheumatol* 17:380–384.
37. Arbabi Ghahroudi M, Desmyter A, Wyns L, Hamers R, Muyldermans S (1997) Selection and identification of single domain antibody fragments from camel heavy-chain antibodies. *FEBS Lett* 414:521–526.
38. Conrath KE, et al. (2001) Beta-lactamase inhibitors derived from single-domain antibody fragments elicited in the camelidae. *Antimicrob Agents Chemother* 45:2807–2812.
39. Otwinowski Z, Minor W (1997) Processing of X-ray diffraction data collected in oscillation mode. *Method Enzymol* 276:307–326.
40. Dodson EJ, Winn M, Ralph A (1997) Collaborative Computational Project, number 4: Providing programs for protein crystallography. *Method Enzymol* 277:620–633.